Edge-Carrier-Assisted Phase Retrieval Receivers Based on Alternative Projections: Performance and Complexity Analysis

Daniele Orsuti[(1,*)], Martina Cappelletti[(1)], Mirko Magarotto[(1)], Marco Santagiustina[(1)], Andrea Galtarossa[(1)], and Luca Palmieri[(1)]

[(1)]Department of Information Engineering, University of Padova, Padova, Italy, [(*)]daniele.orsuti@phd.unipd.it

Abstract *We investigate the performance of edge-carrier-assisted phase-retrieval receivers when using multiple dispersive elements. In relevant simulated transmission settings, the carrier-to-signal power ratio can be as low as -4 dB while incurring a 4-dB OSNR penalty compared to theory at the BER of 3.8e-3. ©2023 The Author(s)*

Introduction

The demand for high-capacity data center interconnects has driven the development of low-cost transceivers capable of achieving data rates $\geq$100 Gb/s/λ over distances of $\sim$100 km using a single span of standard single-mode fiber (SSMF)[1]. Phase retrieval (PR) receivers have recently gained attention for this purpose. They can recover the complex-valued field of an optical signal from intensity-only measurements, eliminating the need for 90-degree optical hybrids and the local-oscillator laser required in standard coherent receivers[2]–[6].

The PR task has been widely investigated in the context of self-coherent (SC) systems[7], where the Kramers-Kronig (KK) has been proposed as an elegant scheme to recover the phase of a single side-band (SSB) minimum-phase signal after single photodiode direct-detection[8]. Yet, the KK receiver requires a carrier-to-signal power ratio (CSPR) higher than 6 dB to achieve the minimum phase condition, which increases the impact of nonlinear fiber propagation effects[9]–[12], and sets stringent requirements on the digital-to-analog converter at transmitter[13]. More recently proposed PR schemes have achieved carrier-less PR retrieval by measuring two (or more) intensity waveforms that are decorrelated by a dispersive element[2],[4],[5]; in these schemes the phase is recovered using a modified version of the Gerchberg-Saxton (GS) algorithm[14]. However, carrier-less PR with the GS algorithm requires 5% to 20% pilot symbols and hundreds of iterations to avoid stagnation in local minima and achieve satisfactory BER performance[2].

To relax the CSPR requirements of SC systems and improve the convergence of iterative PR algorithms, a promising approach is to combine SC transmission with the use of disperse elements[15]–[17]. The leading idea is to use a weak carrier to compute a rough estimate of the true phase (corrupted by signal-to-signal beat interference; SSBI), which can be used to initialize the PR algorithm. This carrier-based initialization approach is similar in concept to using pilot symbols, but it facilitates the convergence of the PR algorithm without reducing the net capacity of the system. Although previous studies have explored the use of carrier-based initialization for PR[15],[16], a comparison between state-of-the-art edge-carrier-assisted (ECA)-PR schemes and their performance when using multiple dispersive elements has not yet been reported.

In this work, we present a comparative analysis between two ECA-PR schemes: the enhanced KK (EKK) scheme, which refines the KK receiver output using nonlinear optimization[15], and the ECA-GS scheme[16], which is based on a modified GS algorithm. Our results show that, compared to EKK, ECA-GS performs better at low CSPR and relaxes the computational requirements. By measuring three intensity waveforms decorrelated by dispersion, we show that the 7% HD-FEC threshold can be achieved after 5-channel WDM transmission (24 GBaud 32-QAM channels) over 100 km of SSMF with a CSPR as low as -4 dB.

System Description

To evaluate the performance of ECA-PR, we consider the 5-channel WDM transmission system shown in Fig. 1(a). Each WDM channel operates at a symbol rate of 24 GBaud with 32-QAM symbols shaped by a raised cosine (RC) pulse with a roll-off factor of 0.05. The channels are spaced by 40 GHz and we evaluate the performance of the central channel. Within each transmitter section, the optical carrier is added virtually[13], exactly at the edge of the information-

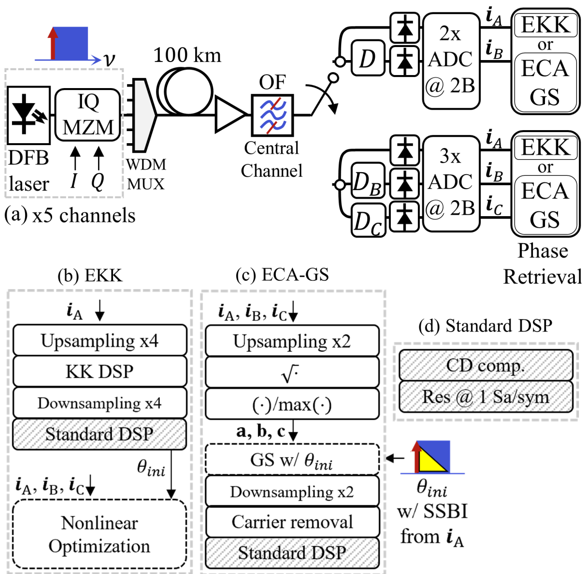

Fig. 1: (a) Simulated 5-channel WDM transmission system; PR-DSP for (b) EKK[15], (c) ECA-GS[16]; (d) Standard DSP.

bearing signal spectrum. The laser source driving the IQ modulator is centered at 1550 nm and has a linewidth of 1 MHz[18]; the IQ modulator is biased at the null-point and the digital-to-analog converter operates without quantization or bandwidth limitations. The optical fiber link consists of a single span of 100 km-long SSMF with dispersion coefficient 17 ps/nm/km, nonlinearity coefficient 1.3 $\mathrm{W}^{-1}\mathrm{km}^{-1}$, and loss 0.2 dB/km. The EDFA at the output of the fiber has a 5 dB noise figure and compensates for the fiber link losses. The employed optical filter (OF) has a 12-th order super-Gaussian shape with 36 GHz bandwidth[8], and selects the central channel. To analyze the performance in presence of multiple dispersive elements, the filtered optical signal is fed to a PR receiver with either one dispersive element, D, or two dispersive elements, D_B and D_C. To ensure a fair performance comparison, when employing a single dispersive element, we set D=-($|D_B| + |D_C|$). We selected D_B=-1445 ps/nm and D_C=+714 ps/nm to introduce enough symbol mixing at each dispersed plane and enough diversity among the intensity measurements; these applied dispersion values are comparable to those used in other related works[4],[16]. Note that D_B and D_C have opposite signs, which was found to be beneficial for improving the convergence speed of the PR algorithms. The PIN photodiodes have 29 GHz electrical bandwidth, and the detected intensity waveforms are digitized by ADCs with 8-bit vertical resolution and sampling rate $2B$, where B is the information signal bandwidth after RC shaping. The ADCs outputs are processed by either

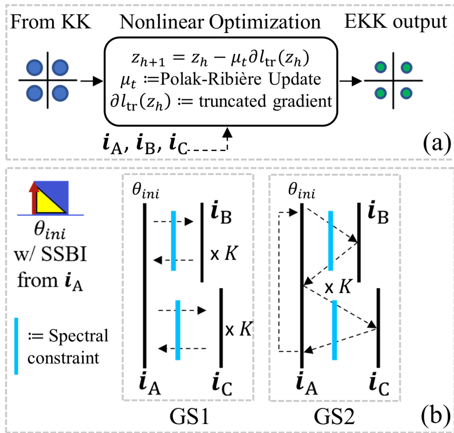

Fig. 2: (a) Nonlinear optimization block entailed in EKK[15],[19]; (b) ECA-GS with two different iteration methods, GS1 and GS2, across the dispersed planes[4].

EKK [Fig. 1(b)] or ECA-GS [Fig. 1(c)] to recover the full-field. The EKK scheme applies KK-DSP to $\boldsymbol{i}_A$ and uses the output symbols to initialize the nonlinear optimization problem defined by Eq. (3) in Ref.[15] [see Fig. 2(a)]. The ECA-GS scheme applies a SSB filtering operation to $\boldsymbol{i}_A$ to initialize the GS algorithm [see Fig. 2(b)]. We implement two versions of the GS algorithm, which iterate differently among the dispersed planes[4]. The first version, GS1, runs K iterations over the first dispersed plane before moving to the next one. The second version, GS2, iterates through the projections sequentially. For each estimated BER point we transmit 50 sequences of 2^{11} symbols.

Results and Discussion

To analyze the convergence properties of EKK and ECA-GS, we evaluated the mean absolute phase error, $\langle|\Delta\theta|\rangle$, versus iteration number, between the transmitted signal and the recovered signals. The results are shown in Fig. 3, where we plot the performance when using either one (D) or two (D_B & D_C) dispersive elements. The OSNR

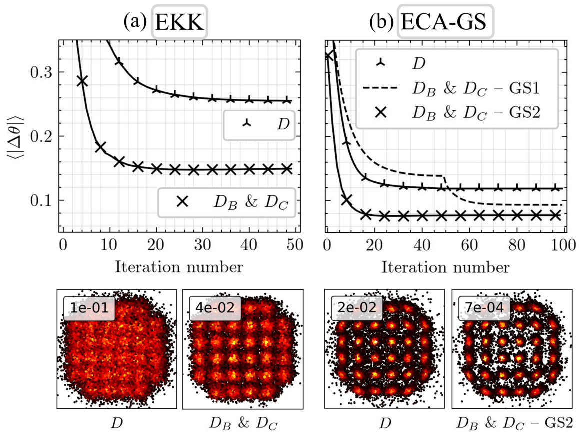

Fig. 3: Mean absolute phase error versus iteration number for (a) EKK and (b) ECA-GS. The reconstructed constellation diagrams at convergence are shown on the bottom (BER is shown on top left corner). The WDM setup parameters are: OSNR 27 dB and CSPR -4 dB.

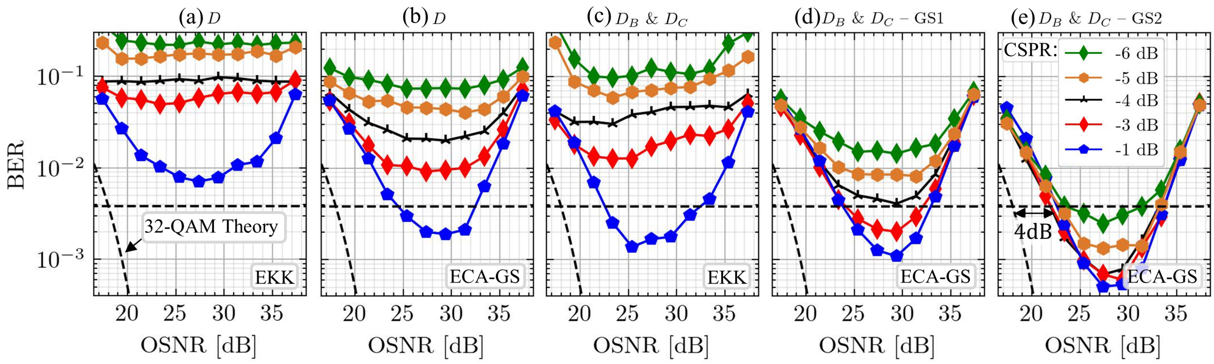

Fig. 4: BER versus OSNR for the CSPRs in the legend after 5-channel WDM transmission over 100 km of SSMF for a 24 GBaud 32-QAM signal (central channel performance). At high OSNR, nonlinear impairments dominate BER degradation. (a) and (b) performance using one dispersive element (D); (c)-(e) performance using two dispersive elements (D_B & D_C).

is set to 27 dB and the CSPR is set to -4 dB. Both EKK and ECA-GS perform better with two dispersive elements due to higher information diversity, which reduces the chances for the iterative PR algorithms getting trapped in local minima. It is evident that ECA-GS outperforms EKK by achieving lower $\langle|\Delta\theta|\rangle$ values with a lower number of iterations. The superior performance of ECA-GS compared to EKK are due to the different phase initializations (SSB filtering vs KK output) and to the adverse impact of noise and propagation-related impairments on the nonlinear optimization algorithm entailed in EKK. Interestingly, when ECA-GS is implemented with the iteration method GS2, it offers the best performance among all the considered PR schemes, achieving the lowest $\langle|\Delta\theta|\rangle$ value with only $\sim$ 20 iterations.

Figure 4(a)-(e) shows the BER versus OSNR performance. With one dispersive element, both EKK [Fig. 4(a)] and ECA-GS [Fig. 4(b)] fail to achieve the 7% HD-FEC threshold for CSPRs lower than -1 dB. This is because the initial phase is strongly corrupted by SSBI at low CSPR values, causing the PR algorithms to converge to a sub-optimal solution. Both EKK [Fig. 4(c)] and ECA-GS [Figs. 4(d) and (e)] achieve better BER performance with two dispersive elements; notably, ECA-GS with the iteration method GS2 achieves the 7% HD-FEC threshold at a CSPR of -4 dB while incurring a 4 dB OSNR penalty compared to an ideal coherent receiver impaired only by AWGN, outperforming all the other schemes.

Computational Complexity Comparison

The complexity of the EKK scheme can be written as $C_{\mathrm{EKK}} = C_{\mathrm{KK}} + C_{\mathrm{NL}}$, where C_{KK} and C_{NL} are the number of real multiplications per sample required by the KK receiver and by the nonlinear optimization algorithm, respectively. The KK complexity is known from previous work[20], whereas C_{NL} can be approximated as $C_{\mathrm{NL}} = 4K \cdot 2 \cdot (N_I \cdot N_{\mathrm{RC}})$, where the factor 4 converts from complex multiplications to real multiplications, K is the number of iterations, the factor 2 accounts for the number of gradient evaluations in each iteration, N_I is the number of measured intensity constraints (N_I=3), and N_{RC}=127 is the number of taps of the RC pulse[15], which has been selected to achieve satisfactory pass-band and stop-band performance. In ECA-GS, each GS iteration between two dispersed planes involves three FFT/IFFT pairs, and the application of two intensity constraints. We assume overlap-save processing with FFT size N=1024, and 50% save ratio[21], i.e., N_{ovlp}=$N/2$, which gives $C_{\mathrm{ECA\text{-}GS}} = 4KRN_I\left[3\left(N\log_2 N + N\right)/\left(N - N_{\mathrm{ovlp}} + 1\right) + 2\right]$, where R=2 is the upsampling factor to accommodate the spectral broadening introduced by the square root operation. The ratio $C_{\mathrm{EKK}}/C_{\mathrm{ECA\text{-}GS}}$ gives that EKK is ~75% more complex than ECA-GS.

Conclusions

We investigated the performance of ECA-PR using multiple intensity measurement decorrelated by dispersion and compared two PR schemes: a nonlinear optimization-based scheme and a GS-based scheme. The GS-based scheme is less computationally expensive and achieves superior performance at a remarkably low CSPR of -4 dB. The results show that ECA-PR with alternative projections is a promising solution to develop low-cost transceivers for high-capacity data center interconnects.

Acknowledgements

This work received partial support from the European Union under the Italian National Recovery and Resilience Plan (NRRP) of NextGenerationEU, partnership on ”Telecommunications of the Future” (PE0000001 - program ”RESTART”) and MIUR (PRIN 2017, project FIRST).

References

[1] K. Zhong, X. Zhou, J. Huo, C. Yu, C. Lu, and A. P. T. Lau, "Digital signal processing for short-reach optical communications: A review of current technologies and future trends", *Journal of Lightwave Technology*, vol. 36, no. 2, pp. 377–400, 2018. DOI: 10.1109/JLT.2018.2793881.

[2] H. Chen, N. K. Fontaine, J. M. Gene, R. Ryf, D. T. Neilson, and G. Raybon, "Dual polarization full-field signal waveform reconstruction using intensity only measurements for coherent communications", *Journal of Lightwave Technology*, vol. 38, no. 9, pp. 2587–2597, 2020. DOI: 10.1109/JLT.2020.2978052.

[3] Y. Yoshida, T. Umezawa, A. Kanno, and N. Yamamoto, "Phase-retrieving coherent reception and its sample complexity", in *2020 European Conference on Optical Communications (ECOC)*, 2020, pp. 1–4. DOI: 10.1109/ECOC48923.2020.9333318.

[4] H. Chen, H. Huang, N. K. Fontaine, and R. Ryf, "Phase retrieval with fast convergence employing parallel alternative projections and phase reset for coherent communications", *Opt. Lett.*, vol. 45, no. 5, pp. 1188–1191, Mar. 2020. DOI: 10.1364/OL.385435. [Online]. Available: https://opg.optica.org/ol/abstract.cfm?URI=ol-45-5-1188.

[5] H. Chen, N. K. Fontaine, H. Huang, R.-J. Essiambre, M. Mazur, R. Ryf, and D. T. Neilson, "Phase retrieval receivers based on alternative projections for coherent optical communications", in *2021 European Conference on Optical Communication (ECOC)*, 2021, pp. 1–4. DOI: 10.1109/ECOC52684.2021.9606011.

[6] E. S. Chou, H. Srinivas, and J. M. Kahn, "Phase retrieval-based coherent receivers: Signal design and degrees of freedom", *Journal of Lightwave Technology*, vol. 40, no. 5, pp. 1296–1307, 2022. DOI: 10.1109/JLT.2021.3130651.

[7] X. Chen, S. Chandrasekhar, and P. Winzer, "Self-coherent systems for short reach transmission", in *2018 European Conference on Optical Communication (ECOC)*, 2018, pp. 1–3. DOI: 10.1109/ECOC.2018.8535234.

[8] A. Mecozzi, C. Antonelli, and M. Shtaif, "Kramers-kronig coherent receiver", *Optica*, vol. 3, no. 11, pp. 1220–1227, Nov. 2016. DOI: 10.1364/OPTICA.3.001220. [Online]. Available: https://opg.optica.org/optica/abstract.cfm?URI=optica-3-11-1220.

[9] Z. Li, M. Erkilinc, K. Shi, E. Sillekens, L. Galdino, B. Thomsen, P. Bayvel, and R. Killey, "Joint optimisation of resampling rate and carrier-to-signal power ratio in direct-detection kramers-kronig receivers", in *2017 European Conference on Optical Communication (ECOC)*, 2017, pp. 1–3. DOI: 10.1109/ECOC.2017.8346206.

[10] X. Chen, C. Antonelli, S. Chandrasekhar, G. Raybon, A. Mecozzi, M. Shtaif, and P. Winzer, "Kramers-kronig receivers for 100-km datacenter interconnects", *Journal of Lightwave Technology*, vol. 36, no. 1, pp. 79–89, 2018. DOI: 10.1109/JLT.2018.2793460.

[11] D. Kong, E. P. da Silva, Y. Sasaki, K. Aikawa, F. Da Ros, M. Galili, T. Morioka, H. Hu, and L. K. Oxenloewe, "909.5 tbit/s dense sdm and wdm transmission based on a single source optical frequency comb and kramers-kronig detection", *IEEE Journal of Selected Topics in Quantum Electronics*, vol. 27, no. 2, pp. 1–8, 2021. DOI: 10.1109/JSTQE.2020.3024004.

[12] D. Orsuti, C. Antonelli, A. Chiuso, M. Santagiustina, A. Mecozzi, A. Galtarossa, and L. Palmieri, "Deep learning-based phase retrieval scheme for minimum-phase signal recovery", *Journal of Lightwave Technology*, vol. 41, no. 2, pp. 578–592, 2023. DOI: 10.1109/JLT.2022.3219639.

[13] M. v. d. Hout, S. van der Heide, and C. Okonkwo, "Kramers-kronig receiver with digitally added carrier combined with digital resolution enhancer", *Journal of Lightwave Technology*, vol. 40, no. 5, pp. 1400–1406, 2022. DOI: 10.1109/JLT.2022.3142353.

[14] R. W. Gerchberg, "A practical algorithm for the determination of phase from image and diffraction plane pictures", *Optik*, vol. 35, pp. 237–246, 1972.

[15] L. Blech, C. Antonelli, A. Mecozzi, Y. C. Eldar, and M. Shtaif, "Enhancing the kramers-kronig receiver via dispersion-based spatial diversity", *Opt. Lett.*, vol. 45, no. 13, pp. 3494–3497, Jul. 2020. DOI: 10.1364/OL.393514. [Online]. Available: https://opg.optica.org/ol/abstract.cfm?URI=ol-45-13-3494.

[16] Q. Wu, Y. Zhu, and W. Hu, "Carrier-assisted phase retrieval", *Journal of Lightwave Technology*, vol. 40, no. 16, pp. 5583–5596, 2022. DOI: 10.1109/JLT.2022.3179838.

[17] D. Orsuti, M. Cappelletti, M. Santagiustina, A. Galtarossa, and L. Palmieri, "Edge-carrier-assisted Phase-Retrieval Based on Deep Learning Enabling low CSPR and low Applied Dispersion Values", in *2023 Optical Fiber Communications Conference and Exposition (OFC)*, San Diego, CA, USA, 2023, pp. 1–3.

[18] W. Yi, Z. Li, M. S. Erkilinc, D. Lavery, E. Sillekens, D. Semrau, Z. Liu, P. Bayvel, and R. I. Killey, "Performance of kramers-kronig receivers in the presence of local oscillator relative intensity noise", *Journal of Lightwave Technology*, vol. 37, no. 13, pp. 3035–3043, 2019. DOI: 10.1109/JLT.2019.2909683.

[19] G. Wang, G. B. Giannakis, and Y. C. Eldar, "Solving systems of random quadratic equations via truncated amplitude flow", *IEEE Transactions on Information Theory*, vol. 64, no. 2, pp. 773–794, 2018. DOI: 10.1109/TIT.2017.2756858.

[20] T. Bo and H. Kim, "Toward practical kramers-kronig receiver: Resampling, performance, and implementation", *Journal of Lightwave Technology*, vol. 37, no. 2, pp. 461–469, 2019. DOI: 10.1109/JLT.2018.2869733.

[21] H. Chen, N. K. Fontaine, M. Mazur, L. Dallachiesa, Y. Zhang, H. Huang, D. van Veen, V. Houtsma, A. Blanco-Redondo, R. Ryf, and D. T. Neilson, "140g/70g direct detection pon $>$37 db power budget and 40-km reach enabled by colorless phase retrieval full field recovery", in *2021 European Conference on Optical Communication (ECOC)*, 2021, pp. 1–4. DOI: 10.1109/ECOC52684.2021.9605860.